Soil Science

Environmental and Applied Aspects

Volume II

Brian Bechdal

Soil Science: Environmental and Applied Aspects Volume II

Edited by **Brian Bechdal**

CALLISTO REFERENCE
New York

Published by Callisto Reference,
106 Park Avenue, Suite 200,
New York, NY 10016, USA
www.callistoreference.com

Soil Science: Environmental and Applied Aspects
Volume II
Edited by Brian Bechdal

International Standard Book Number: 978-1-63239-569-6 (Hardback)

Printed in China.

Preface

Environmental soil science is a wide area of study, which discusses the interaction of humans with the various layers of atmosphere such as pedosphere, biosphere, lithosphere and hydrosphere. Environmental soil science directly targets the fundamental as well as applied aspects such as surface water quality and buffers, vadose zone functions, land treatment and wastewater, stromwater, erosion related aspects, contamination of soil by metals and chemicals used in pesticides, remedies of soil contamination, degradation of soil, nutrients management techniques and developments and movement of different bacteria in the soil and water. Also included in this field are studies related to acid rains, land usage and global warming.

In contemporary times, the human civilisation is facing a lot of problems. Overpopulation happens to be a major cause of worry for a lot of countries. This is resulting in an extreme pressure on all our resources such as water, air, fuel etc. Feeding such a huge population is also an issue. In such a scenario, environmental soil science is the need of the hour. This is also because soil plays a crucial role in maintaining the various ecosystems which exist on Earth.

Instead of organizing the book into a pre-formatted table of contents with chapters, sections and then asking the authors to submit their respective chapters based on this frame, the authors were encouraged by the publisher to submit their chapters based on their area of expertise. The editor was then commissioned to examine the reading material and put it together as a book.

This effort would not have been possible without the kind cooperation of our contributors who patiently went through revisions of their chapters. I convey my heartfelt thanks to all the contributors and to the team at the publishing house for their encouragement and excellent technical assistance as and when required. I hope that this book will contribute significantly to both the basic and advanced group of readers, who are engaged in studies related to Environmental soil science.

Editor

Contents

The Effect of Dissolved Humic Acids on Aluminosilicate Formation and Associated Carbon Sequestration

Ashaki A. Rouff,[1] Brian L. Phillips,[2] Stacey G. Cochiara,[2] and Kathryn L. Nagy[3]

[1] *School of Earth and Environmental Sciences, Queens College CUNY, Flushing, NY 11367, USA*
[2] *Department of Geosciences, Stony Brook University, Stony Brook, NY 11794, USA*
[3] *Department of Earth and Environmental Sciences, University of Illinois at Chicago, Chicago, IL 60607, USA*

Correspondence should be addressed to Ashaki A. Rouff, ashaki.rouff@qc.cuny.edu

Academic Editor: Teodoro Miano

Allophane and imogolite neogenesis in soils may occur in the presence of organic matter. To understand this process under conditions relevant to soils, the influence of dissolved organic carbon (DOC) as humic acid (HA), on aluminosilicate formation was studied at 25°C, pH 6, and low-DOC concentrations. For solutions with initial Al/Si ratios of 1–2.1, and 0–6 mg/L DOC, precipitates recovered after 20 h had Al/Si ratios of 2.2–2.7. The formation of allophane, imogolite-like material, and aluminosilicate gel was confirmed by XRD, FTIR, and NMR. The effect of DOC was to produce a small, but systematic increase in imogolite-like Si in the precipitate, and a decrease in the formation of aluminosilicate gel. Results suggest that the presence of DOC as HA slows the otherwise rapid polymerization of Al and Si at low temperature, and may also promote the formation of imogolite. The high C content of these precipitates indicates that this process may facilitate the sequestration of organic matter, slowing C cycling in soils.

1. Introduction

Complexation of Al with natural organic matter is important for the development of soils, influencing both the weathering and neogenesis of Al-bearing minerals [1] including aluminosilicate clays. The metastable clay minerals allophane and imogolite, when present, may control the solubility of both Al and Si relative to more stable phases such as gibbsite and kaolinite [2]. Allophane and imogolite are poorly crystalline hydroxyaluminosilicates with Al/Si ratios ranging from 0.5–4. They are composed of Si and Al polyhedral layers shaped into hollow tubes and spheres [3]. Imogolite, $(OH)_3Al_2O_3SiOH$ [4], which has long-range order, is tubular in shape and has an Al/Si ratio of 2. Allophane has short-range order and forms hollow spherules with a range of Al/Si ratios. Al-rich allophane is also called protoimogolite or imogolite-like allophane and has an Al/Si ratio of ~2 [4]. Imogolite and allophane occur frequently as, but are not limited to, what are termed allophanic horizons in volcanic soils such as andisols and spodosols [5]. Their occurrence is contingent upon conditions such as soil pH, the availability of sufficient Si, and the presence of organic material, which can either inhibit the formation of [5], or conversely, stabilize these minerals [6]. The large surface area and high reactivity of these minerals promote complexation with organic matter [6], the essential soil nutrients P and N, and toxic contaminants such as As, Cd, Cu, and Pb [7, 8].

Laboratory synthesis of aluminosilicate phases in the presence of organic constituents has been previously explored. Organic additives such as quercetin [9] and organometalloid reagents such as aluminum-sec-butoxide (ASB) and tetraethoxysilane (TEOS) [10, 11] were used to synthesize aluminosilicates including kaolinite, halloysite, allophane, and imogolite. The specific phases that formed and their amounts depended on factors such as initial Al/Si ratio, pH, temperature, and aging time. The proposed precipitation mechanism involves the slowing of Al hydroxide polymerization by formation of stable Al-organo complexes.

These complexes are thought of as precursor species that have Al–O (and possibly Si–O) bonds required for attachment of alumina and silicate sheets [12]. This eliminates the need for conversion of Al–OH to Al–O bonds in systems predisposed to Al hydroxide precipitation and facilitates the formation of required Al–O–Si linkages with the organic material acting as a "catalyst" which is subsequently recycled. Conversely, addition of organic acids such as citric [13] and more complex, naturally occurring fulvics and humics [14] were observed to inhibit the formation of well-defined phases during synthesis at 96–100°C. The concentration of imogolite declined with increasing organic concentration, eventually giving way to the formation of only disordered aluminosilicates and pseudoboehmite [13, 14]. However, to be applicable to natural systems synthesis at low temperature is required. Uniquely, this study was conducted at 25°C to systematically explore the effect of dissolved organic carbon (DOC) from natural humic acid (HA) on the formation of aluminosilicate minerals. Results isolated the role of initial chemical composition on aluminosilicate formation, as a first step in deconvoluting the complexity of this process in natural soils.

2. Experimental Details

Stock solutions for batch experiments were prepared by diluting in deionized water (DI) 1000 mg/L Al in HNO_3, and 1000 mg/L Si in DI standard solutions. Suwannee River Humic Acid (SRHA, International Humic Substances Society) containing 53 wt % C was dissolved in DI water to produce a 250 mg/L DOC stock. Though a river humic acid was chosen for this study, the carboxylic content can be similar to that of soil humic acids. A matrix of experimental binary and ternary solutions was prepared with variable Al, Si, and DOC concentrations (Table 1). Appropriate amounts of the stock solutions were mixed in the sequence Si and/or Al stock solution followed by DOC stock solution to yield a total volume of 80 mL. Solution pH was adjusted to a value close to 6 (±0.5 pH unit) using <0.5 mL 0.1 or 1.0 M NaOH, and initial concentrations were corrected for this addition. Time-series data indicated that aqueous concentrations of all components in filtered (0.2 μm PTFE syringe filters) mixed solutions were invariant after 20 h; thus, all experiments were conducted for this time period. Solutions were stirred only during preparation and prior to filtration. Aqueous Al and Si concentrations were determined by Inductively Coupled Plasma-Optical Emission Spectroscopy (ICP-OES) using a Perkin Elmer Optima 4300 instrument. All solutions were prepared and sampled in duplicate.

2.1. Thermodynamic Calculations. Based on results from small-volume batch experiments, solutions with select concentrations of Al, Si, and DOC were chosen to generate large amounts of precipitates for subsequent analysis (Table 1). The initial aqueous speciation and saturation states with respect to potential solid precipitates were calculated using Visual MINTEQ ver 2.53 with the Thermo.vdb database [15]. For all calculations, initial concentrations of Al, Si, and DOC were entered, along with any base required for pH adjustment. The pH was calculated from the charge and mass balance in solution prior to precipitation, that is, the H^+ concentration was adjusted until the charge difference was ≤0.01%. For DOC-bearing solutions, the Stockholm Humic Model (SHM) [16] was used to model metal-humic complexation. Acid dissociation constants for SRHA carboxylic and phenolic functional groups available from IHSS [17] were included.

Table 1: Concentrations of Al, Si, and DOC used for binary and ternary experiments (variable [DOC]), variables [Si] and [Al], and experiments used to generate precipitates for further analysis).

	Al (mM)	Si (mM)	DOC (mg/L)
Binary solutions	—	0.3	6
	0.3	—	6
	0.3	0.3	—
Ternary solutions: variable [DOC]	0.3	0.3	3
	0.3	0.3	6
	0.3	0.3	9
Variable [Si]	0.3	0.05–1.5	—
	0.3	0.05–1.5	6
Variable [Al]	0.05–1.5	0.3	—
	0.05–1.5	0.3	6
Solutions for precipitate recovery	0.5	0.5	—
	0.5	0.5	6
	0.75	0.5	—
	0.75	0.5	6
	1.0	0.5	—
	1.0	0.5	6

2.2. Evaluation of Precipitate Phases. Experiments designed to generate sufficient material for compositional and mineralogical analysis (Table 1) were prepared in an 800 mL volume in triplicate and were treated with <1 mL 10 N NaOH for pH adjustment. After 20 h, each solution was vacuum-filtered using a 0.2 μm polycarbonate filter, the filtrate sampled for Al and Si analysis, and the precipitate recovered. The final mass of precipitate was placed in a drying oven at 40°C for several hours to expedite evaporation of excess moisture, then ground gently using a mortar and pestle. A portion of sample was dissolved using 0.1 M HNO_3 and the Al and Si concentrations determined by ICP-OES analysis. Total C content was determined using a Carlo Erba 2500 CHNS Elemental Analyzer. X-ray diffraction (XRD) data were collected from 2–65° 2-theta with a step size of 0.02° using a Siemens D5000 X-ray diffractometer. Fourier transform infrared (FTIR) spectroscopy data were collected in transmission mode for samples in a KBr background using a Perkin Elmer Spectrum 100 spectrometer.

Both ^{29}Si and ^{27}Al nuclear magnetic resonance spectroscopy (NMR) data were collected for generated solids. The ^{29}Si single-pulse magic angle spinning (SP/MAS) and $^{29}Si\{^1H\}$ cross-polarization magic angle spinning

(CP/MAS) spectra were collected with a 400 MHz (9.4 T) Varian Inova spectrometer operating at 79.5 MHz for ^{29}Si using a Varian/Chemagnetics T3 sample probe assembly configured for 3.2 mm (o.d.) rotors. The SP/MAS spectra were collected under quantitative acquisition conditions using a 90° pulse (5 μs) and 180 s relaxation delay at a spinning rate of 10 kHz. The CP/MAS spectra were obtained at spinning rates of 5 and 10 kHz using a ramp of the transverse ^{1}H field during polarization transfer for contact times ranging from 0.5 to 15 ms. For the ^{27}Al SP/MAS NMR spectra, a 500 MHz (11.7 T) Varian Infinity Plus spectrometer was used, operating at 130.3 MHz with the sample spinning at 18 kHz in 3.2 mm rotors. The acquisition parameters consisted of 1.0 μs pulses (π/12) and a 1.0 s relaxation delay, which correspond to uniform excitation and full relaxation of the central transition. Additional spectra were taken for the 1.0 mM Al samples at 217 MHz (19.5 T; Center for Interdisciplinary Magnetic Resonance, National High Magnetic Field Laboratory, Tallahassee, FL, USA). These high-field spectra were taken at a 10 kHz spinning rate (4 mm spinning system) under low-power conditions using 4 μs pulses and 0.5 s relaxation delay for a total of 128 acquisitions.

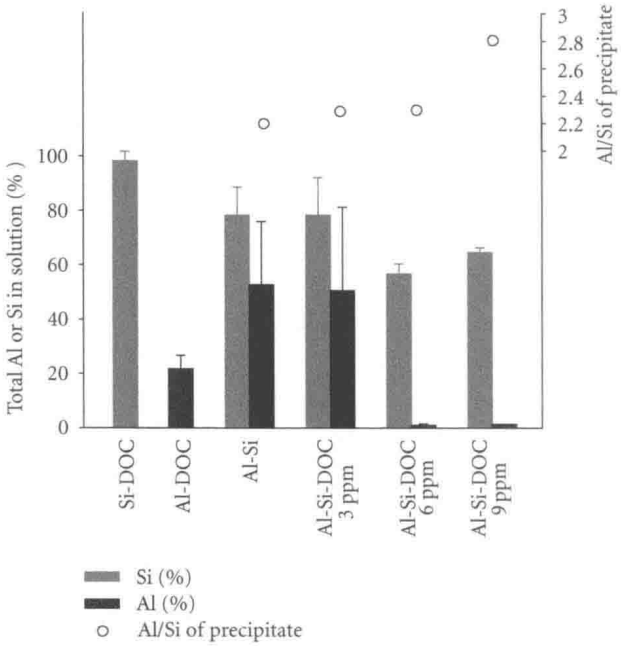

FIGURE 1: Percentage of total aqueous Al and Si in solution (bars) and Al/Si ratio (open symbols) for binary and ternary solutions with Al = Si = 0.3 mM and 0–9 mg/L DOC.

3. Results

3.1. Al and Si Removal from Binary and Ternary Solutions. Results for ternary Al-Si-DOC and binary Al-Si, Al-DOC and Si-DOC experiments show that for all systems, Si is less susceptible to removal from the aqueous phase relative to Al (Figure 1). Comparison of results from the binary Al-Si, Si-DOC, and Al-DOC experiments indicates that aqueous Si concentration is reduced in the presence of Al but not DOC, whereas Al is removed from solution in the presence of Si, and to a greater extent in the presence of DOC.

Equal amounts of Al and Si precipitated from Al-Si solutions with 0 or 3 mg/L DOC. As DOC concentration increased from 3 to 6 mg/L, removal of both Al and Si was enhanced. At 9 mg/L DOC no additional Al was removed, and aqueous Si concentrations increased slightly, relative to the 6 mg/L DOC solution. These results suggest that removal of both Al and Si was optimized in the 6 mg/L DOC solution relative to binary and other ternary solutions, therefore 6 mg/L DOC was used in subsequent experiments in which initial concentrations of Al and Si were varied. The Al/Si ratios of precipitates from 0, 3, and 6 mg/L DOC solutions are 2.2-2.3, suggesting that precipitates formed both in the absence and presence of DOC may be similar in composition. The slightly higher Al/Si ratio of 2.8 in precipitates from 9 mg/L DOC solutions suggests the precipitation of additional Al, possibly caused by the higher concentration of DOC.

Comparing the results from binary and ternary systems indicates that in the latter Al may precipitate both as aluminosilicate and alumino-organic complexes. As Si does not appear to form insoluble complexes with DOC, enhanced Si removal in Al-Si-DOC solutions, with DOC > 3 mg/L, relative to Al-Si solutions appears to result by the formation of aluminosilicate complexes which may bind to the DOC by an Al-bridging mechanism (i.e., Si-Al-DOC). Coprecipitation of aluminosilicate with precipitating organics may also occur. Hence, significant reduction in both Al and Si concentrations in Al-Si-DOC solutions is likely caused by multiple complexation and precipitation pathways.

3.2. The Effect of Varying Al or Si Concentration in Solutions with 0 or 6 mg/L DOC. The effect of variable Si concentration from 0.05 to 1.5 mM Si was evaluated at a fixed initial Al concentration of 0.3 mM and fixed DOC concentration of 0 or 6 mg/L. The amount of Si remaining in solution after 20 h was slightly below the initial value in all cases with no obvious effect of DOC (Figure 3(a)). The final concentration of Al remained much lower than the initial value regardless of initial Si, with a slightly higher value (less removal) only at 1.5 mM Si (Figure 3(b)). Below 0.3 mM initial Si, aqueous Al concentration remained slightly higher for Al-Si relative to Al-Si-DOC solutions. This is consistent with the enhanced removal of Al in DOC solutions.

The effect of variable Al concentration from 0.05 to 1.5 mM was evaluated at an initial Si concentration fixed at 0.5 mM, a value anticipated to be sufficient for observing potential interactions with the higher concentrations of Al. Total Si concentration decreased with increasing initial Al (Figure 3(c)), with comparable behavior for 0 and 6 mg/L DOC solutions except from 0.6 to 0.9 mM initial Al where the final Si concentration of the Al-Si solutions without DOC increased abruptly (Figure 3(c)). A similar abrupt increase occurred for final Al in the same Al-Si solutions (Figure 3(d)). In the Al-Si-DOC solutions, the Si concentration abruptly increased at 1 mM initial Al (Figure 3(c)) to a value similar to that of the DOC-free solution. In

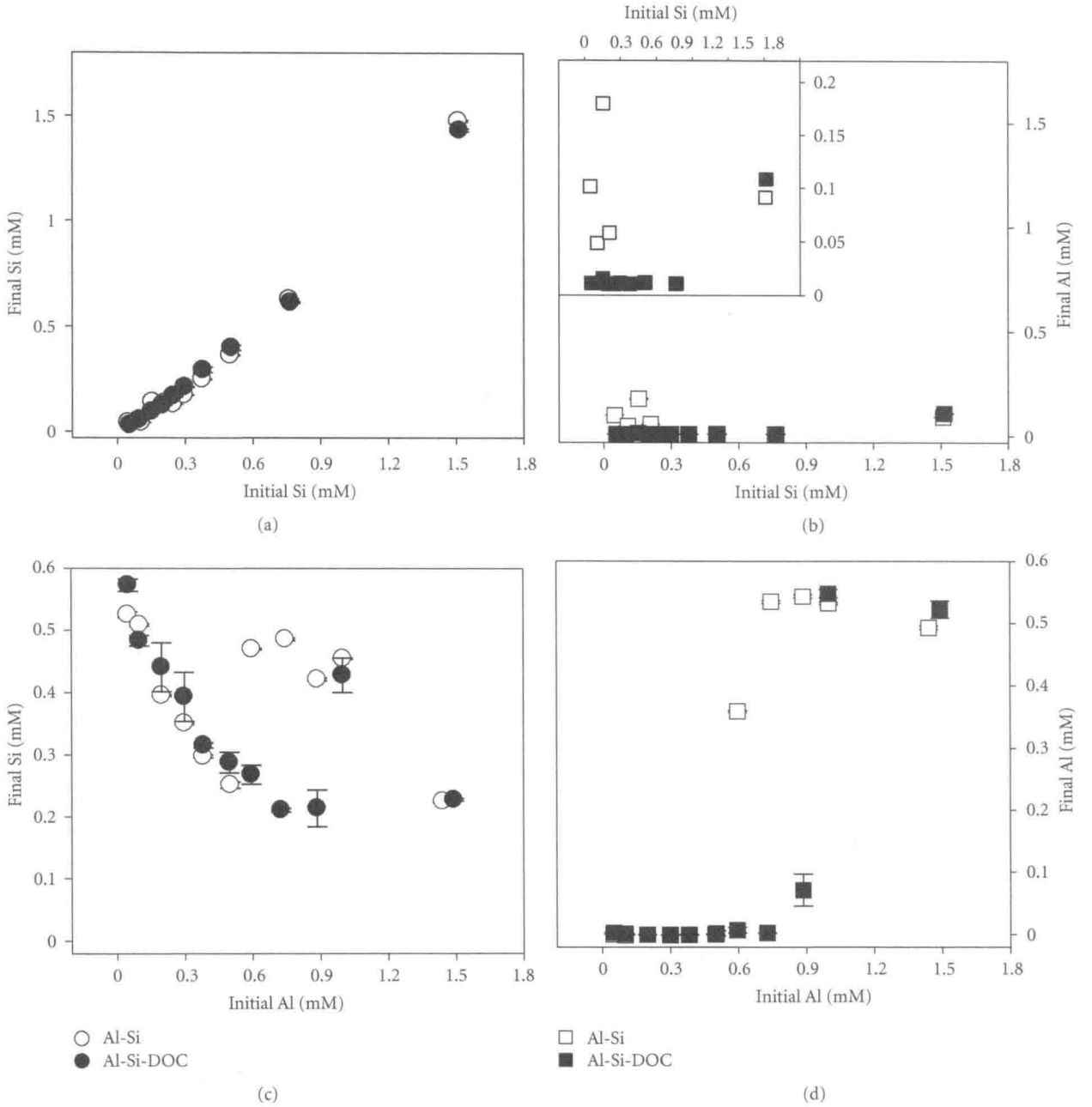

FIGURE 2: Final concentrations of (a) Si and (b) Al for 0.05–1.5 mM Si, 0.3 mM Al; (c) Si and (d) Al at 0.05–1.5 mM Al, 0.5 mM Si; in Al-Si (0 mg/L DOC) and Al-Si-DOC (6 mg/L DOC) solutions.

these solutions, Al concentration fell rapidly to a low value and remained relatively constant up to 1 mM initial Al (Figure 3(d)), above which it also increased to values similar to those in the DOC-free solution.

Solids recovered from Al-Si and Al-Si-DOC solutions with 0.5, 0.75, and 1.0 mM initial Al were analyzed to investigate further the deviation between Al-Si and Al-Si-DOC systems observed over the initial Al concentration range of 0.6–1.0 mM.

3.3. Speciation in and Saturation States of Initial Solutions Containing 0.5, 0.75, and 1.0 mM Al, 0.5 mM Si, and 0 or 6 mg/L DOC. Thermodynamic modeling was used to estimate initial aqueous speciation and predicted precipitates for the 0.5, 0.75, and 1.0 mM Al solutions with 0.5 mM Si and 0 or 6 mg/L DOC. The dominant initial aqueous Al and Si species are $Al(OH)_2^+$ and $H_4SiO_4^0$ (Table 2). With increasing Al concentration, the concentration of $AlH_3SiO_4^{2+}$ complexes increases subtly. The fraction of polymeric $Al_3(OH)_4^{5+}$ increases by a factor of 10 when the

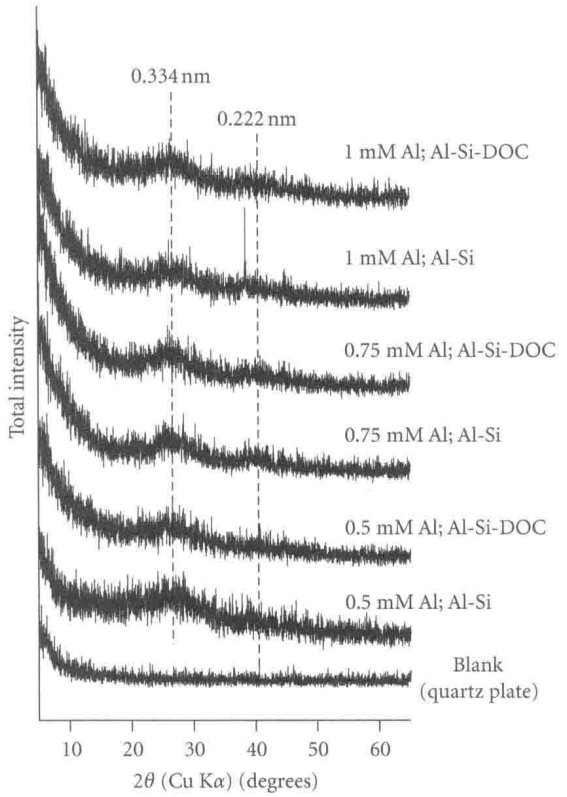

FIGURE 3: X-ray diffraction patterns for solids derived from Al-Si and Al-Si-DOC solutions with 0.5, 0.75, and 1.0 mM Al; 0.5 mM Si; 0 or 6 mg/L DOC.

initial Al concentration is doubled from 0.5 to 1.0 mM. For initial Al-Si-DOC solutions, the overall fractions of dominant species, $Al(OH)_2^+$, $Al(OH)_3^0$ and $Al(OH)_4^-$, are somewhat lowered relative to those in Al-Si solutions, but otherwise the speciation trends are similar. Speciation of Al as the aluminum tridecamer Al_{13} was negligible as formation of this species is limited in the presence of Si [18] and HA [19]. The calculated pH for all solutions ranged from pH 6.03 to 6.09, consistent with the measured pH of 6.00 ± 0.5 for all samples.

The predicted species for Al complexed with SRHA are primarily bidentate HA_2AlOH and HA_2Al^+ along with a small fraction (<1%) of electrostatically bound Al. The fraction of Al-HA complexes decreases with increasing initial Al concentration; however, the absolute concentration of Al complexed to HA, including electrostatic species, is ~0.027 mM for all initial Al concentrations (Table 2). The concentration of DOC involved in this complexation is about 0.053 mM, corresponding to 0.6 mg/L or one-tenth of the initial DOC in solution.

The ^{13}C NMR analysis of SRHA [23] indicates that 15% of the C occurs as carboxyl functional groups. For 6 mg/L (0.5 mM) DOC solutions approximately 0.07 mM of C would be associated with these groups. If Al complexes primarily with carboxyl functional groups [24], then the maximum concentration of C available for complexation with Al is 0.07 mM. Thus, the thermodynamic calculations suggest that ~70% of this C (0.05 mM) may be directly bonded to Al to form bidentate Al-HA complexes in solution.

The supersaturated mineral phases for all initial Al-Si and Al-Si-DOC solutions are kaolinite, halloysite, imogolite, allophane, diaspore, boehmite, gibbsite, amorphous $Al(OH)_3$, and quartz. All solutions were undersaturated with respect to amorphous SiO_2. Though thermodynamically feasible, not all predicted phases will precipitate under the given solution conditions. For example, spontaneous precipitation of quartz is likely only in supersaturated solutions [25] well above the concentrations studied here, whereas that of diaspore is rare in the absence of stabilizing substituting ions such as Fe [26].

3.4. Precipitates from Initial Solutions with 0.5, 0.75, and 1.0 mM Al, 0.5 mM Si, and 0 or 6 mg/L DOC. Solids formed from the Al-Si solutions were white to colorless, whereas those from Al-Si-DOC solutions were dark brown, similar in color to the initial solutions. All precipitates were gel-like in consistency. Of Al, Si, and C, Al was highest in concentration by weight (wt %) in all samples (Table 3) and was highest for the samples formed in initial 0.75 mM Al solutions with and without DOC. The wt % Si decreased with increasing initial Al concentration for solids formed in Al-Si solutions and was highest in the solid formed in the 0.75 mM Al-Si-DOC solution. The wt % C in the solids also decreased with increasing initial Al consistent with the corresponding decrease in the calculated fraction of Al-HA complexes and suggesting that these complexes are precursors to Al-HA precipitates in the solids.

Precipitates from 0.5 mM initial Al solutions that contained DOC had less mass (58 mg), Al, and Si than precipitates (72 mg) from the solutions without DOC. The Al/Si mole ratio for the precipitates was 2.2. The mole ratio of Al/C in the precipitate from the DOC-bearing solution was 0.7. The lower mass of the Al-Si-DOC solids suggests that Al-HA complexation inhibits or slows the formation of aluminosilicate phases, but does not change the bulk inorganic composition of the precipitate compared to DOC-free solutions. If the HA is a simple coprecipitate in the solids, it would be associated with about 1 wt% of the precipitated Al, assuming the same bidentate stoichiometry with carboxyl groups as in the soluble Al-HA species. This would lower the Al/Si ratio in the inorganic precipitate to ~2.

At 0.75 mM initial Al, again the total mass of precipitate from the Al-Si solution was greater (190 mg) compared to the mass (169 mg) precipitated from the Al-Si-DOC solution. The fraction of precipitated Al and Si is higher in the Al-Si-DOC solid compared to the Al-Si solid, but the Al/Si ratio is the same within uncertainty. This Al/Si ratio is, however, slightly higher than the ratios in the 0.5 mM Al precipitates. Assuming an Al/Si mole ratio of 2 in the inorganic part of the precipitate, the excess Al is too high by a factor of ~8 to be solely in the form of bidentate Al-HA complexes, assuming there is no fractionation (i.e., selective precipitation of smaller molecules with higher proportions of Al-binding sites) of the HA during precipitation. This suggests that a small amount of an Al-(oxy)hydroxide phase may have

Table 2: Speciation of Al and Si in 0.5, 0.75, and 1.0 mM Al; 0.5 mM Si solutions with 0 (Al-Si) and 6 mg/L (Al-Si-DOC) as calculated using Visual MINTEQ ver 2.53 with the Thermo.vdb database[1].

Al-Si	Si species percent		Al species percent									
[Al] mM	$H_4SiO_4^0$	$AlH_3SiO_4^{2+}$	$Al(OH)_2^+$	$Al(OH)_3^0$	$Al(OH)_4^-$	$AlOH^{2+}$	Al^{3+}	$Al_3(OH)_4^{5+}$	$AlH_3SiO_4^{2+}$			
0.5	98.1	1.8	48.9	23.0	14.6	9.0	0.9	1.6	1.8			
0.75	96.9	3.1	48.5	20.5	11.8	10.2	1.2	5.3	2.1			
1	96.0	4.0	46.0	19.0	11.0	10.1	1.3	10.0	2.0			
Al-Si-DOC	Si species percent		Al species percent								mM	
[Al] mM	$H_4SiO_4^0$	$AlH_3SiO_4^{2+}$	$Al(OH)_2^+$	$Al(OH)_3^0$	$Al(OH)_4^-$	$AlOH^{2+}$	Al^{3+}	$Al_3(OH)_4^{5+}$	$AlH_3SiO_4^{2+}$	Al-HA	Al-HA	C
0.5	98.1	1.9	47.2	21.1	12.6	9.2	1.0	1.6	1.9	5.3	0.026	0.052
0.75	96.9	3.1	47.2	19.1	10.6	10.4	1.3	5.3	2.1	3.5	0.027	0.053
1	95.9	4.0	45.0	18.0	10.1	10.2	1.3	10.0	2.0	2.7	0.027	0.053

[1]Source of thermodynamic data for aqueous species: Al hydrolysis species [20]; $AlH_3SiO_4^{2+}$ [21]; $Al_3(OH)_4^{5+}$ [22]. Organic complexation was calculated using the Stockholm Humic Model [16].

Table 3: Composition of precipitates derived from solutions with initial 0.5, 0.75, and 1.0 mM initial Al; 0.5 mM initial Si and 0 or 0.5 mM (6 mg/L) DOC.

	Al-Si					Al-Si-DOC							
	Initial		Precipitate			Initial			Precipitate				
[Al] mM	Al/Si[1]	Mass[2] (mg)	Al wt percent	Si wt percent	Al/Si[1]	Al/Si[1]	Al/C[1]	Mass[2] (mg)	Al wt percent	Si wt percent	C wt percent	Al/Si[1]	Al/C[1]
0.5	1	72	22.7	10.9	2.2	1	1	58	17.9	8.6	12.0	2.2	0.7
0.75	1.5	190	23.3	9.2	2.6	1.5	1.5	169	25.9	9.8	9.3	2.7	1.2
1	2.1	142	20.3	9.0	2.3	2	2	182	20.2	7.8	5.2	2.7	1.7

[1]Mole ratios.
[2]Uncertainty is ± 1 mg.

formed as predicted by the thermodynamic calculations. DOC appears to promote aluminosilicate precipitation, but the overall composition of the precipitate is similar to that of DOC-free solids.

At 1.0 mM initial Al, the mass of precipitate (142 mg) from the Al-Si solutions was less than that (182 mg) from the Al-Si-DOC solutions. The wt% of precipitated Al is the same for both DOC-free and DOC-bearing solids, but less than that for solids formed from solutions with initial Al of 0.75 mM. The Al/Si ratio of the Al-Si-DOC sample is similar to that of the solids formed in the initial 0.75 mM Al solutions. However, the Al/C ratio indicates less precipitated C relative to the 0.5 and 0.75 mM samples, which correlates with the decrease in the calculated fraction of Al-HA complexes in solution with increasing initial Al. Again, assuming an Al/Si ratio in the aluminosilicate of 2 and no fractionation of the HA during precipitation, the excess precipitated Al is about a factor of 6 too high to be complexed only to carboxyl C in coprecipitated HA suggesting the formation of a minor amount of Al-(oxy)hydroxide.

3.4.1. XRD Analysis. X-ray powder diffraction patterns show that all solids exhibited low crystallinity, with no notable differences as a function of Al concentration or in the absence or presence of DOC (Figure 2). Broad peaks centered at approximately 0.334 nm and 0.222 nm, characteristic of allophane [6, 7, 27], occur in all samples. Aluminum-rich allophanes ($Al_2O_3 \cdot xSiO_2 \cdot yH_2O$ ($x = 1$; $y = 2$–5)) classified as protoimogolite or imogolite-like allophane [28] can have Al/Si ratios ranging from 2.3 to 2.7 [29], consistent with the observed range of 2.2 to 2.7. The observed XRD reflections are also common to imogolite, although there are additional imogolite reflections [30, 31] that are absent in the XRD patterns. The additional peaks are also significantly less intense than the observed peaks and would be close to background in these samples. Thermodynamic calculations indicated initial supersaturation with respect to allophone, imogolite, halloysite, and kaolinite. However, equilibration of halloysite and kaolinite is slow at room temperature [2, 12], whereas allophane readily forms in oversaturated solutions [31].

3.4.2. FTIR Analysis. Sample spectra reveal bands at ~3500, 970, 570, and 430 cm^{-1}, characteristic of allophane and imogolite [8, 32] (Figure 4). The diffuse band at 3000–3800 cm^{-1} is indicative of OH stretching of Al–OH, Si–OH, and water [33], with an additional water band at ~1600 cm^{-1}. The peak at 970 cm^{-1} is attributed to Si–O

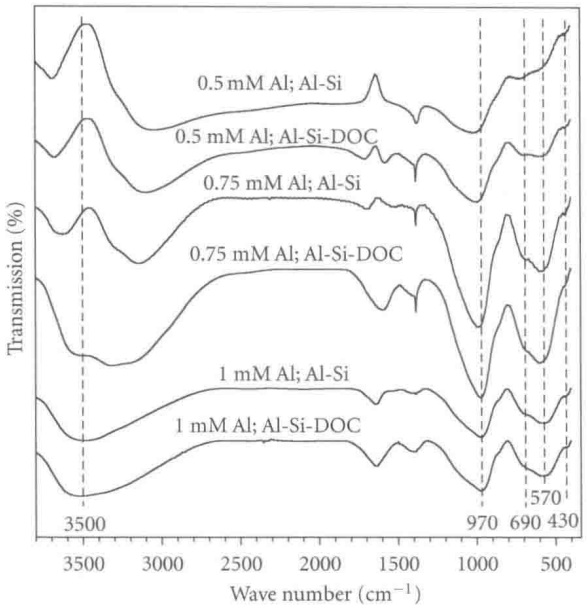

FIGURE 4: FTIR spectra for solids derived from Al-Si and Al-Si-DOC solutions with 0.5, 0.75 and 1.0 mM Al; 0.5 mM Si; and 0 or 6 mg/L DOC.

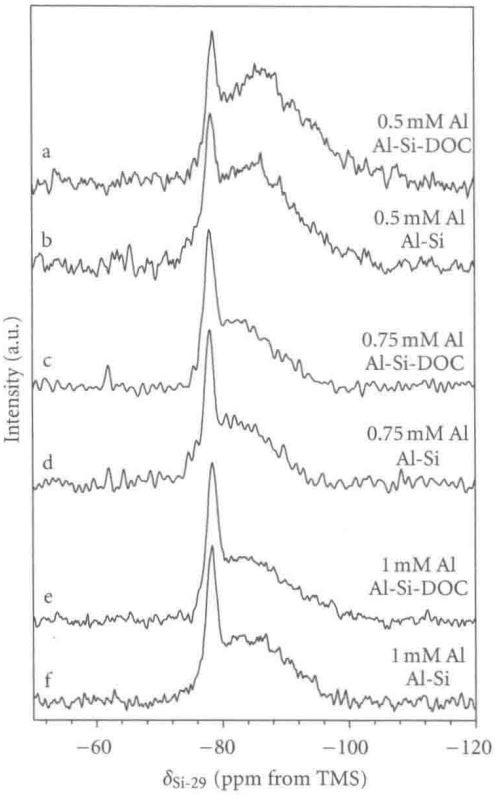

FIGURE 5: ^{29}Si SP/MAS NMR spectra of precipitates from solutions with 0.5 mM Si and (a-b) 0.5 mM Al; (c-d) 0.75 mM Al; (e-f) 1.0 mM Al; with and without 6 mg/L DOC as indicated. All spectra were taken under quantitative conditions with a 180 s relaxation delay and 10 kHz spinning rate.

stretching and shifts to higher wavenumbers at lower Al/Si ratios with the peak for 0.5 mM initial Al samples closer to 1000 cm^{-1}. The peaks in the 800–400 cm^{-1} range are from Si–O–Al and Si–O–Si stretching. The broad band at 570 cm^{-1} with shoulders at 690 and 430 cm^{-1} indicates an imogolite-like structure observed in natural allophane and imogolite [27]. Compared to allophane, imogolite peaks are sharper with doublets at 970 and 570 cm^{-1} [32, 34]. Sharper peaks for 0.75 mM initial Al solids may indicate more imogolite or imogolite-like material in these samples. The broadest peaks are observed for the 0.5 mM initial Al solid with no DOC, indicative of less imogolite-like material in this sample.

3.4.3. NMR Analysis. The ^{29}Si SP MAS/NMR spectra of all the precipitates contain a narrow peak at a chemical shift of $\delta_{Si\text{-}29} = -78.3$ ppm (1.8 ppm full width at half maximum; FWHM) plus a broad signal at more negative chemical shifts that can be represented by two broad peaks, near −82 ppm and −89 ppm, and 9–17 ppm FWHM, in varying proportions (Figure 5). The narrow peak is characteristic of imogolite-like Si environments, in which a silicate tetrahedron is coordinated to three 6-coordinated Al ions and one hydroxyl ion [35, 36]. The broad peaks arise from polymerized Si, and resemble closely those reported previously for natural allophane [36, 37] and also for synthetic hydroxy-aluminosilicates [38, 39]. For the precipitates from solutions with 0.75 mM initial Al, (Figures 5(c) and 5(d)) the imogolite-like environments represent a greater proportion of the Si (20–23%) than for those with 1.0 mM initial Al (18–21%; Figures 5(e) and 5(f)) and 0.5 mM initial Al (10%; Figures 5(a) and 5(b); Table 4). For solids from 0.75 mM and 1.0 mM solutions, the fitted intensity of the imogolite-like peak is somewhat higher for the Al-Si-DOC relative to the Al-Si samples. Although the difference is subtle, the values for Al-Si-DOC samples are consistently higher than those of Al-Si samples (Table 4). For all pairs of Al-Si/Al-Si-DOC samples, the average chemical shift of the broad component was slightly more negative by 1-2 ppm for the Al-Si-DOC solids suggesting an increased tetrahedral Si/Al ratio in the polymerized structures. The ^{29}Si{^{1}H} CP/MAS spectra (not shown) are essentially identical to the corresponding SP/MAS spectra except for some minor differences in relative intensity, which varied only slightly with the NMR experimental contact time.

The aluminosilicate precipitates have ^{27}Al MAS/NMR spectra that contain peaks centered near 5.5, 33, and 59 ppm, which are characteristic of Al in 6-, 5-, and 4-coordination, respectively (Figure 6). These values are the observed peak positions at 11.7 T. The peaks for 4- and 6-coordinated Al (Al^{IV} and Al^{VI}) are similar to those reported for natural imogolite and allophane [29, 36] and for synthetic amorphous hydroxyaluminosilicates [38]. In addition to Al^{IV} and Al^{VI}, a peak for 5-coordinated Al (Al^{V}) from allophane similar to that observed here has been reported [40] but would have been difficult to detect at the slower spinning rates used in the earlier studies. The integrated intensities of the three resonances were estimated by fitting the center

Table 4: The percentage of imogolite-like Si from ^{29}Si NMR, corresponding to the integrated relative intensity of the peak at −78.3 ppm. The $\delta_{Si\text{-}29}$ of the gel component is the weighted average of the broad signal, excluding the imogolite-like peak. Also reported is the percentage of Al in 4-, 5-, and 6-fold coordination from ^{27}Al NMR.

Sample	^{29}Si NMR		^{27}Al NMR		
	Imogolite-like Si percent	$\delta_{Si\text{-}29}$ gel	$Al^{(IV)}$ percent	percent $Al^{(V)}$	$Al^{(VI)}$ percent
0.5 mM Al-Si	10	−85.7	18	5	77
0.5 mM Al-Si-DOC	10	−87.9	16	5	79
0.75 mM Al-Si	20	−83.1	24	5	71
0.75 mM Al-Si-DOC	23	−84.0	16	5	79
1.0 mM Al-Si	18	−84.6	26	5	69
1.0 mM Al-Si-DOC	21	−85.8	22	5	73

bands to lineshapes calculated from a random distribution of electric field gradients [41]. These simulations reproduce well the characteristic peak shapes, particularly the broad tail extending to lower chemical shifts most evident in the peak for Al^{VI}. The best-fit lineshape parameters (Table 4) varied only slightly among the samples: $\delta_{iso} \approx 7.9 \pm 0.3$ ppm and mean quadrupolar coupling constant, $Cq = 2.8$ MHz for Al^{VI}; $\delta_{iso} \approx 63 \pm 1$ ppm and $Cq = 4.2$ MHz for Al^{IV}; $\delta_{iso} \approx 36 \pm 1$ ppm for Al^{V}. An average Cq value of 4.2 MHz was used to fit the Al^{V} peak shape, which gave a constant relative intensity of 5% for all samples. These values are in reasonable agreement with high-field (217 MHz) spectra obtained for the 1.0 mM Al samples (Figures 6(g) and 6(h)), which give peak positions at 62.0, 34.0, and 6.0 ppm.

The 1.0 mM Al samples (Figures 6(e) and 6(f)) contain a lower proportion of Al^{VI} (69–73%) and larger proportion of Al^{IV} (22–26%) relative to other samples. The 0.75 mM samples (Figures 6(c) and 6(d)) contain 71–79% Al^{VI} and 16–24% Al^{IV} and the 0.5 mM samples (Figures 6(a) and 6(b)) 77–79% Al^{VI} and 16–18% Al^{IV} (Table 4). Small, but systematic, increases in the Al^{VI}/Al^{IV} ratios were noted for samples precipitated with HA (Figures 6(a), 6(c), 6(e), and 6(g)) corresponding to 2–8% more Al^{VI} compared to the samples precipitated from binary Al-Si solutions. In each case, the decrease in Al^{IV} fraction correlates with a more negative chemical shift for the broad ^{29}Si component, consistent with a decrease in the average number of Al^{IV} bonded to polymerized Si. Other than these minor changes in relative intensity, virtually no difference in the ^{27}Al spectra of samples coprecipitated with DOC was observed compared to those from HA-free solutions.

Results from ^{29}Si MAS/NMR indicate the presence of both short-range ordered imogolite-like structures plus more polymerized Si environments, which is typical of allophane. The highest fraction of imogolite-like Si is observed in the 0.75 mM solids, consistent with inferences from FTIR analysis. Results from ^{27}Al MAS/NMR also indicate the presence of Al^{IV} in all samples. Tetrahedral Al is typically not observed in natural and synthetic imogolite phases [29, 39], and its occurrence along with that of polymerized Si suggests the presence of allophane or aluminosilicate gel [36]. For natural allophanes with Al/Si 2.3–2.70, the ratio of Al^{IV}/Al^{total} is typically 0.015–0.04 (1.5–4% Al^{IV}) as determined by ^{27}Al MAS/NMR [29]. Assuming that Al^{IV}/Al^{total} ratios are close to those of natural samples or synthetic imogolite-like allophane, Al^{IV} concentrations in our samples are higher than expected if allophane was the only constituent. This result suggests that some fraction of Al^{IV} could be associated with polymerized Si in a separate amorphous hydrated aluminosilicate gel in these samples.

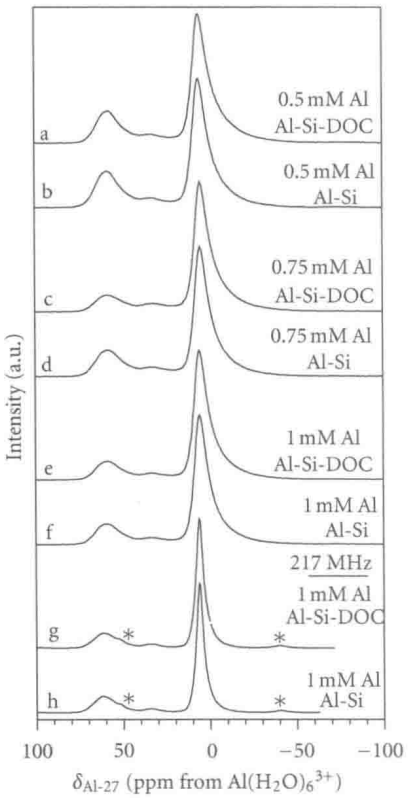

Figure 6: ^{27}Al MAS/NMR spectra of precipitates from solutions with 0.5 mM Si and (a-b) 0.5 mM Al; (c-d) 0.75 mM Al; (e–h) 1.0 mM Al; with and without 6 mg/L DOC as indicated. All spectra taken with SP excitation at 130.3 MHz (11.7 T) and 18 kHz spinning rate, except (g-h) obtained at 217 MHz (19.5 T), spinning at 10 kHz. Asterisks denote spinning sidebands.

Although the presence of an amorphous Al-(oxy)hydroxide cannot be ruled out, such materials generally contain lower Al^{IV}/Al^{VI} ratios than observed here. It should be noted that the role of Al^{IV} and polymerized Si in allophane remains uncertain, with some evidence that these signals arise from an impurity in natural allophane [42]. The Al^{V} that is observed for all samples could represent an intermediate product in the transition between allophane and imogolite which involves transformation of Al^{IV} to Al^{VI} [39]. The presence of Al^{V} and the apparent coexistence of several phases demonstrate the transitional nature of these samples. The NMR data provide evidence for a mixture of imogolite-like structures, allophone, and aluminosilicate gel in all samples, with the fractions of both imogolite-like environments and Al^{IV} increasing with increasing initial Al concentration. For solids generated in the presence of HA, consistently lower Al^{IV}/Al^{VI} ratios combined with more imogolite-like Si suggest less aluminosilicate gel formed in these systems.

4. Discussion

4.1. Al-Si Systems. In the experimental solutions, Si should have been dominantly monomeric (pH < 9; [Si] < 2-3 mM) [43], a form thought to have a low affinity for Al, and as a consequence Al-(oxy)hydroxide phases are expected to polymerize relatively rapidly [44]. However, the precipitates have low Al/Si ratios implying limited polymerization of separate Al-(oxy)hydroxide phases and instead enhanced formation of allophane and aluminosilicate gel.

The formation of poorly crystalline aluminosilicates in Al-Si solutions agrees with previous observations. For example, the Al/Si ratios of the initial solutions and precipitated solids for the 0.5 mM and 1.0 mM Al-Si samples are similar to those observed for pH 4.0–4.5 solutions aged for 7 years at 25°C [45]. Despite higher pH and shorter aging times, the current precipitates are compositionally similar to and thus may be the precursors of these precipitates [45]. The consistently higher fractions of imogolite-like Si observed in 0.75 and 1.0 mM Al-Si-DOC solids show that over short reaction times dissolved organic matter promotes the formation of imogolite-like material.

4.2. Al-Si-HA Systems. At pH 6 HA is soluble, deprotonated, and thus able to complex with Al, which otherwise polymerizes rapidly [12]. Organics are known to inhibit Al polymerization, depending upon the affinity of the ligand for Al [46–48]. Because HA has a strong affinity for Al, polymerization is reduced, and the formation of amorphous Al phases is promoted [49, 50], as indicated by the thermodynamic modeling of the initial compositions of the experimental solutions. As Si alone also reduces Al polymerization, and the number of Al-HA binding sites is limited, Al-(oxy) hydroxide polymerization is further reduced in the presence of both Si and HA.

Precipitates in HA-bearing systems contain a significant portion of organic matter, suggesting insoluble metal-organo complexes. In pH 5-6, Si-free, Al-HA solutions, this can be attributed to chelation, sorption of humics on $Al(OH)_3$ flocs, and/or coprecipitation mechanisms [51]. The addition of Si and subsequent detection in the precipitate suggests that these mechanisms involve aluminosilicate material. Results from experiments with only Si and HA show no independent interaction of these two components. This is because Si prefers to be tetrahedrally coordinated and so forms weak complexes with HA carboxylic functional group oxygens, compared to the stable five-membered chelate rings that readily form with Al [52]. Because Si-HA complexation is negligible, any interaction of Si with HA is likely to proceed indirectly. Thus, the precipitation mechanisms for Si may involve insoluble Al-bridged Si-Al-HA complexes.

At low initial HA concentrations (~12 mg L^{-1} HA) and at 25°C for short reaction times (20 h), pure imogolite did not dominate the precipitate at any of the solution Al/Si ratios. However, concentrations of HA > 300 mg L^{-1} appeared to inhibit imogolite formation from solutions with Al/Si ratios of 2, heated to 96–100°C and aged for up to 110 hours [14]. Below this threshold pure imogolite was observed as the only detectable precipitate phase. The lower temperatures and shorter aging times in the current work are not conducive to the formation of pure imogolite, and therefore the role of HA is notably different from that reported previously. Results also suggest that any inhibitory effect of HA is shifted to lower concentrations relative to the published experimental results at higher temperature and much longer reaction time. For example, for 0.5 mM initial Al samples the presence of HA reduced the quantity of precipitate to a small extent. Though concentrations >12 mg L^{-1} HA were not used to generate solids for further analysis, observations from experiments with ~18 mg L^{-1} HA (9 mg/L DOC) suggest that more Al preferentially binds to the organics resulting in less Al-Si complexation and a reduction in aluminosilicate solid formation under these conditions. This may be interpreted as a slight inhibitory effect of HA on aluminosilicate formation at higher HA concentrations. On the other hand, the effect of HA on some solids characterized in this study was to produce a small but detectable increase in the production of imogolite-like material relative to aluminosilicate gel in comparison to HA-free systems.

4.3. Relation to Natural Soil Systems. The studied conditions apply to those that may be observed in natural systems for allophane- and imogolite-bearing horizons of some andisols and spodosols. These soils are typically characterized by low DOC concentrations, pH on the order of 5–6.5, and sufficient Si to promote imogolite formation [5]. Current results show that although allophane can be produced in organic-free solutions, organic matter seems to promote the formation of imogolite-like structures when present in low concentrations. These structures in turn may be precursors to a pure imogolite phase. Organic matter may thus play an active role in the formation of both allophane and potentially imogolite in soils, which becomes evident in natural soils with high organic content. In some volcanic andisols, allophane production can be limited by enhanced Al-humic complexation, as observed for 0.5 mM Al solids,

termed an antiallophanic process [53]. However, this apparent inhibitory effect does not apply to all soils as high organic C coinciding with high allophane content has been observed for some Argentinean andisols [54] and tropical volcanic soils [6]. In the latter case, allophane and imogolite have a high capacity to store organic matter thus stabilizing and slowing C cycling in soils. In the current study, this is alluded to by the high C content of the 0.75 mM initial Al-Si-DOC solid, combined with the highest fraction of imogolite-like material relative to solids from other experiments. Results also indicate the importance of Al/Si and Al/C ratios in this process. In addition, Basile-Doelsch et al. [6] observed that organic matter formed chelates with allophane, inhibiting the formation of more crystalline phases such as feldspars and gibbsite. The stabilizing effects of organics on aluminosilicate phases may in turn explain the subtle, but systematic preference for more imogolite-like material in HA-bearing samples in the current study. Here, Al-HA binding might increase the production of amorphous aluminosilicate minerals by slowing not only Al-polymerization, but aluminosilicate polymerization which would otherwise increase the fraction of gel-like material, as observed in HA-free solutions. Hence, organic matter may stabilize and promote the formation of imogolite-like material, which can in turn facilitate the sequestration and storage of organic matter. This has implications for global warming and associated climate change, whereby enhanced soil weathering and productivity with increasing temperature can accelerate the production of allophanic soils which in turn can increasingly sequester organic carbon. In natural systems, the observed disparities in the role of organic material in allophane and imogolite synthesis may be attributed to factors such as parent material and climate, which are critical during soil formation processes [6]. In turn, these factors can dictate Al/Si and Al/C ratios in soil systems, which are based on results of the current study, determining the role of organic material in allophane and imogolite neogenesis.

5. Conclusions

Solids with Al/Si ratios ranging from 2.2–2.7 were formed from solutions with 0.5, 0.75, and 1.0 mM initial Al, and aqueous Al/Si and Al/C ratios of 1, 1.5, and 2. Allophane was the dominant mineral in all solids, with the fraction of imogolite-like Si and aluminosilicate gel depending on initial solution composition. At 0.5 mM initial Al, the presence of HA did not significantly affect the composition of the precipitate or the fraction of imogolite-like material. At higher initial Al, formation of imogolite-like structures was enhanced, with slightly higher fractions observed in DOC-bearing solids, and the highest fraction for a solid formed from a solution of 0.75 mM Al, 0.5 mM Si, and 6 mg/L DOC. The amount of aluminosilicate gel increased with increasing initial Al concentration, but was reduced in the presence of HA.

Results of this study demonstrate the influence of HA on the formation of aluminosilicates under conditions applicable to certain soil systems. Allophane and imogolite-like material were successfully synthesized at ambient conditions in short reaction times, both in the presence and absence of HA at environmentally relevant concentrations of Al, Si, and DOC. Both Si and HA limit, if not prevent, the polymerization of Al-(oxy)hydroxide phases. HA further limits the polymerization of aluminosilicate gel and has a subtle, but consistent effect on increasing the fraction of imogolite-like material relative to HA-free systems. The influence of HA on the formation of poorly crystalline aluminosilicates, contingent upon initial Al/Si and Al/C ratios, along with a stabilizing effect of the mineral on the organic phase via chelation or coprecipitation, may explain the coincidence of allophanic soil horizons with organics in some soil systems. This in turn has implications for C storage and sequestration.

Acknowledgments

Dr. Zhehong Gan, National High Magnetic Field Laboratory is thanked for collecting the high-field ^{27}Al NMR spectra. Funding is gratefully acknowledged from the National Science Foundation through the Grant EAR-0455938 from the University of Illinois at Chicago.

References

[1] G.F. Vance, F. J. Stevenson, and F. J. Sikora, "Environmental chemistry of aluminum-organic complexes," in *The Environmental Chemistry of Aluminum*, G. Sposito, Ed., pp. 169–220, Lewis, Boca Raton, Fla, USA, 1995.

[2] H. Bilinski, L. Horvath, N. Ingri, and S. Sjoberg, "Aluminosilicate phases during initial clay formation: H^+-Al^{3+}-oxalic acid-Silicic acid-Na^+ system," *Journal of Soil Science*, vol. 41, no. 1, pp. 119–132, 1990.

[3] K. Wada, "Structure and formation of non- and paracrystalline aluminosilicate clay minerals: a review," in *Clay Controlling the Environment*, G. J. Churchman, R. W. Fitzpatrick, and R. A. Eggleton, Eds., pp. 443–448, CSIRO Publishing, Melbourne, Australia, 1995.

[4] R. L. Parfitt, "Allophane and imogolite: role in soil biogeochemical processes," *Clay Minerals*, vol. 44, no. 1, pp. 135–155, 2009.

[5] F. C. Ugolini and R. A. Dahlgren, "Weathering environments and occurrence of imogolite/allophane in selected Andisols and Spodosols," *Soil Science Society of America Journal*, vol. 55, no. 4, pp. 1166–1171, 1991.

[6] I. Basile-Doelsch, R. Amundson, W. E. E. Stone et al., "Mineralogical control of organic carbon dynamics in a volcanic ash soil on La Réunion," *European Journal of Soil Science*, vol. 56, no. 6, pp. 689–703, 2005.

[7] Y. Arai, D. L. Sparks, and J. A. Davis, "Arsenate adsorption mechanisms at the allophane—Water interface," *Environmental Science and Technology*, vol. 39, no. 8, pp. 2537–2544, 2005.

[8] L. Denaix, I. Lamy, and J. Y. Bottero, "Structure and affinity towards Cd^{2+}, Cu^{2+}, Pb^{2+} of synthetic colloidal amorphous aluminosilicates and their precursors," *Colloids and Surfaces A*, vol. 158, no. 3, pp. 315–325, 1999.